# Perturbed-angular-correlation study of electric quadrupole interactions in nanocrystalline $ZrO_2$

M. Forker
*Universität Bonn, Institut für Strahlen-und Kernphysik, Nussallee 14-16, D-53115 Bonn, Germany*

U. Brossmann and R. Würschum
*Universität Stuttgart, Institut für Theoretische und Angewandte Physik, D-70550 Stuttgart, Germany*

(Received 20 August 1997)

The electric quadrupole interaction (QI) of $^{181}$Ta on Zr sites of nanocrystalline $ZrO_2$ prepared by crystallite condensation, oxidation, and *in situ* compaction was investigated by perturbed-angular-correlation (PAC) measurements which show the existence of three components with different QI parameters. The dominant contribution to the PAC spectra is characterized by a broad distribution of strong axially asymmetric electric-field gradients, suggesting a highly disordered oxygen environment of the Zr sites in the nanocrystallites in addition to a distribution of probe sites in the crystallite interfaces. The other two PAC components correspond to monoclinic and tetragonal $ZrO_2$. The thermal evolution of the phases in nanocrystalline $ZrO_2$ was studied by isochronal annealing between 290 K and 1500 K. The complete transformation of the disordered component to the monoclinic phase requires an annealing temperature of $T_A = 1400$ K, indicating that complete defect recovery occurs only after a martensitic transformation cycle through the high-temperature tetragonal phase. [S0163-1829(98)02509-0]

## I. INTRODUCTION

Nanocrystalline (*n*-)ceramics, e.g., *n*-$ZrO_2$, are currently the subject of comprehensive investigations in view of their improved properties compared to the coarse-grained counterparts, such as ductility and sintering at reduced temperatures (for a recent review see Ref. 1). An assessment of the physical properties of nanocrystalline ceramics requires a detailed structural characterization. For this purpose in particular scattering techniques, as x-ray diffraction (see, e.g., Ref. 2), Raman scattering,[3] extended x-ray-absorption fine structure (EXAFS),[4] and small angle neutron scattering,[5] as well as conventional and high-resolution transmission electron microscopy[6] were applied.

The present paper reports a study of nanocrystalline $ZrO_2$ by means of perturbed angular correlations (PAC). PAC such as Mössbauer spectroscopy, nuclear magnetic resonance, and other techniques of nuclear solid-state physics measures the electric and magnetic hyperfine interaction (HFI) of probe nuclei in condensed matter. Because of the $r^{-3}$ dependence of the HFI, these methods sample charge distributions and spin densities in solids on a nanometer scale and therefore appear particularly well suited for the investigation of nanocrystalline materials (for a recent review see Ref. 7). The number of PAC studies in this field is at present still rather limited. Electric quadrupole interactions (QI's) have been investigated by Sinha and Collins[8] in In nanocrystals, by Wolf *et al.*[9] in nanocomposite WGa and CdS, and by Lauer *et al.*[10] in WGa and ball-milled TiAl. Bai and Collins[11] have studied the QI's on grain boundary sites of fcc metals.

In the present PAC study we have investigated the QI's of the probe nucleus $^{181}$Ta on Zr sites of *n*-$ZrO_2$. The QI parameters of $^{181}$Ta in the monoclinic and tetragonal phase of crystalline $ZrO_2$ are well known.[12] The comparison of these values with the QI parameters of the same probe in *n*-$ZrO_2$ may lead to the identification of the phases present in the nanocrystalline material and provide information on structural defects which are difficult to obtain by scattering techniques. In addition to the nanocrystalline structure after preparation the structural evolution during annealing up to temperatures $T_A = 1500$ K was studied and compared with previous measurements of x-ray diffraction.[2]

## II. EXPERIMENTAL DETAILS AND DATA ANALYSIS

The nanocrystalline $ZrO_2$ specimen was prepared by dc sputtering of Zr with Zr crystallite condensation and collection in an Ar atmosphere of $p = 20$ Pa, as well as subsequent oxidation and *in situ* crystallite compaction (pressure 1.5 GPa) in high vacuum at ambient temperature.[2] This synthesis technique yields well-reproducible particle sizes as confirmed by x-ray-diffraction studies of different samples. The slow oxidation during the preparation results in a complete tetragonal structure.[2] Prior to the PAC study the specimen was sintered at $\sim 625$ K for 1 h in an $O_2$ atmosphere of 300 mbar, giving rise to a mixture of the tetragonal and monoclinic phases with mean crystallite diameters of 10 nm and 17 nm, respectively, as determined by x-ray diffraction using the Scherrer formula (Table I).

The PAC measurements were carried out with the 133–482 keV $\gamma\gamma$ cascade of $^{181}$Ta which is populated in the $\beta$ decay of the 42-*d* isotope $^{181}$Hf. Due to the chemical similarity of Hf and Zr, the Zr targets (Goodfellow metals) used for the specimen preparation contained about 0.13 at. % Hf which is very convenient for the PAC investigation of these compounds. The isotope $^{181}$Hf can be produced by thermal neutron capture in $^{180}$Hf (natural abundance 18.5 at. %): $^{180}\mathrm{Hf}(n,\gamma)^{181}\mathrm{Hf}$. Therefore, doping of Zr compounds with $^{181}$Hf, the mother isotope of the PAC nucleus $^{181}$Ta, is easily achieved by thermal neutron irradiation. In the present case 5 mg of *n*-$ZrO_2$ were neutron irradiated for 50 h in a flux of $5\times10^{13}$ *n*/s cm$^2$.

The neutron-activated *n*-$ZrO_2$ specimen was submitted to

 

TABLE I. Results of the analysis of PAC spectra of $^{181}$Ta on Zr sites of nanocrystalline $ZrO_2$ (see Figs. 1 and 2). The quadrupole frequency $\nu_q$, the asymmetry parameter $\eta$, the relative width $\delta$ of a Lorentzian frequency distribution, and the relative intensity $f_i$ are given for the three components $i$ ($i=1,2,3$) present in the measured spectra. $f_{\text{x-ray}}$ and $d$ denote the fraction and crystallite size of the phases as determined by x-ray diffraction.

| Component | | | $\nu_q$ [MHz] | $\eta$ | $\delta$ | $f$ | $f_{\text{x-ray}}$ | $d$ [nm] |
|---|---|---|---|---|---|---|---|---|
| 1 | broad | as-prepared | 850(50) | 1 | 0.30(5) | ~0.57 | | |
| 2 | monoclinic | as-prepared | 760 | 0.43 | 0.12 | ~0.38 | 0.65(5) | 17 |
| | | $T_A=1400$ K | 802.6(6) | 0.333(3) | 0.03 | 1.0 | 1.0 | (300)[a] |
| 3 | tetragonal | as-prepared | 1200(30) | 0 | 0.02 | ~0.05 | 0.35(5) | 10 |

[a]Obtained from transmission electron microscopy of a reference specimen after annealing at $T_A=1320$ K (Ref. 17).

an isochronal annealing program of 1 h per step in a vacuum of $10^{-5}$ mbar. After each annealing step a PAC spectrum was taken at ambient temperature with a standard four-detector setup equipped with fast $BaF_2$ scintillators. Annealing and measurements were carried out in the PAC setup without removing the sample from its position. A reference measurement was performed on commercial $ZrO_2$ powder (Johnson Matthey) at ambient temperature.

From the PAC spectra information on the electric quadrupole interactions can be derived. The modulation of the angular correlation coefficients $A_{kk}$ ($k=2,4$) of the $\gamma\gamma$ cascade by hyperfine interactions in polycrystalline samples can be described by a perturbation factor $G_{kk}(t)$ which depends on the multipole order, the symmetry, the time dependence, and the spin of the intermediate state of the cascade (for details see, e.g., Frauenfelder and Steffen[13]). In the present paper we are dealing with perturbations by the static electric quadrupole interaction between the nuclear quadrupole moment $Q$ and the tensor of the electric-field gradient (EFG) which can be expressed by two independent quantities, the quadrupole frequency $\nu_q=eQV_{zz}/h$ and the asymmetry parameter $\eta=(V_{xx}-V_{yy})/V_{zz}$, where $V_{ii}$ ($i=x,y,z$) are the principal-axis components of the EFG with $|V_{xx}|\leq|V_{yy}|\leq|V_{zz}|$. Distributions of the QI's caused by structural or chemical defects lead to an attenuation of the oscillatory PAC pattern and are usually described by the relative width $\delta$ of a Gaussian or Lorentzian distribution. In the present case the assumption of Lorentzian distributions was found to give slightly better fits.

PAC spectra arising from nuclei with different QI's are described by an effective perturbation factor $A_{kk}G_{kk}(t)=A_{kk}\Sigma_i f_i G_{kk}(t;\nu_{qi},\eta_i,\delta_i)$ where $f_i$ (with $\Sigma_i f_i=1$) is the relative intensity of the $i$th fraction with the QI parameters $\nu_{qi}$, $\eta_i$, and $\delta_i$. These parameters and the intensities $f_i$ were determined by least-squares fits of the theoretical perturbation factor to the measured PAC spectra. The experimental anisotropy at the time zero point is affected by prompt coincidences from the decay of the radioisotope $^{95}$Zr produced by the neutron irradiation. Therefore the angular correlation coefficient $A_{22}$ was fixed in the analysis for all annealing temperatures to the value obtained from the fit to the spectrum measured after $T_A=1500$ K. Because of the prompt contribution, only the data points with delay times $t>3$ nsec were taken into account.

## III. RESULTS AND DISCUSSION

The PAC spectra measured on $n$-$ZrO_2$ after preparation and annealing as well as the results of the numerical analysis are shown in Figs. 1 and 2, respectively. With increasing annealing temperature $T_A$ the PAC spectra evolve from a strongly attenuated pattern (as-prepared state, Fig. 1) to an oscillatory pattern ($T_A=1225$ K, Fig. 1) which corresponds to the transition of broad QI distributions to sharp QI frequencies.

### A. Structure and defects after preparation

The PAC spectra in the as-prepared state and after annealing at low temperatures can be well described by a superposition of three components (Nos. 1–3) which are characterized as follows (see Table I).

*Component No. 1 (broad QI distribution)*: The dominant contribution (No. 1) to the PAC spectrum arises from a strongly damped oscillation with the hyperfine parameters $\nu_q=850$ MHz, $\eta=1$, and a large relative width $\delta=0.30$ of a Lorentzian distribution. A component with similar QI parameters has been observed in the PAC spectra of zirconia prepared by the sol-gel process.[14] The large frequency distribution which usually also produces a strong EFG asymmetry[15] reflects a high degree of disorder.

*Component No. 2 (monoclinic phase)*: A second component (weak solid line in Fig. 1) in the PAC spectra is attributed to the monoclinic phase since the quadrupole frequency $\nu_q=802.6$ MHz and asymmetry parameter $\eta=0.333$ of this component for $T_A=1400$ K are in perfect agreement with the values of the monoclinic ($m$-)$ZrO_2$ reference specimen (see Fig. 2 and Table I). In the as-prepared state the quadrupole frequency of this component is slightly smaller whereas the asymmetry parameter is substantially larger (~50%) and the frequency distribution is enhanced by a factor of 3–4 compared to coarse-grained monoclinic $ZrO_2$. Similar observations have been made by Sinha and Collins[8] in a PAC study of nanocrystalline In. These deviations can be attributed to the small crystallite diameter $d\simeq 14$ nm in the as-prepared state (see topmost section of Fig. 2). In this case about 20% of the PAC probes are in the two surface-nearest layers where the QI's can be expected to differ from the volume sites of the bulk. Apparently the differences are not large enough to be resolved in the PAC spectra, but the large num-

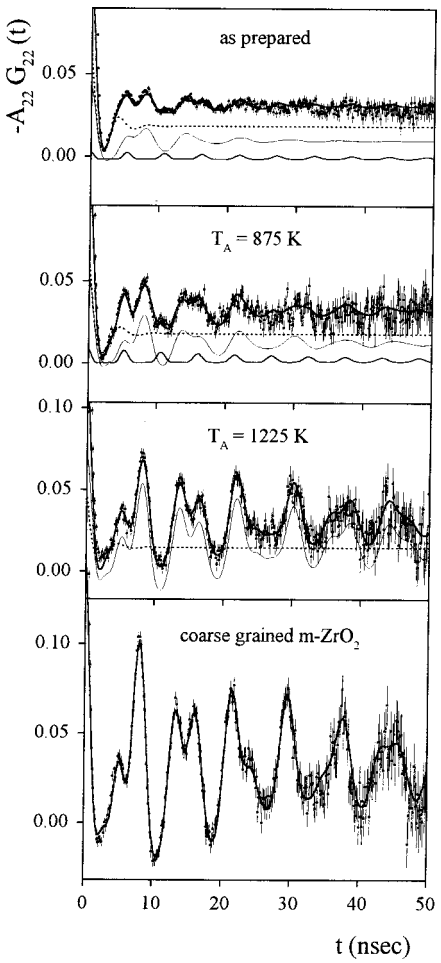


FIG. 1. PAC spectra of $^{181}$Ta in nanocrystalline $ZrO_2$, measured at ambient temperature after neutron activation and consecutive annealing at the temperature $T_A$. The specimen was preannealed at 625 K prior to neutron irradiation. The bottommost section shows the spectrum of $^{181}$Ta measured on a commercial monoclinic $ZrO_2$ powder. The fits and their decomposition into three components are shown (see Table I). The weak solid line corresponds to monoclinic, the strong solid line to tetragonal $ZrO_2$, and the dotted line to the highly disordered fraction.

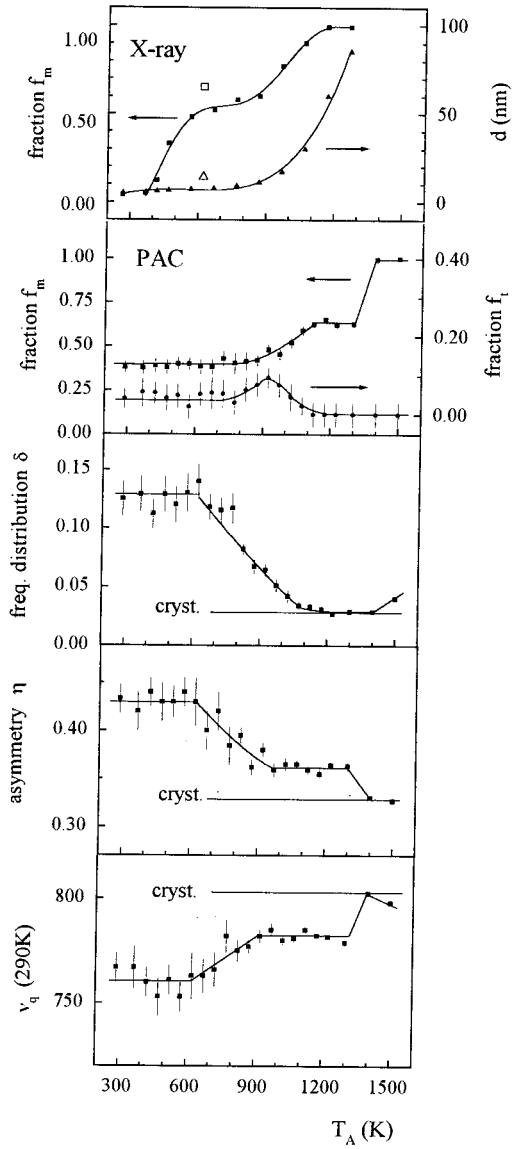


FIG. 2. Quadrupole frequency $\nu_q$, asymmetry parameter $\eta$, relative width $\delta$ of a Lorentzian frequency distribution, and relative intensity $f_m$ of the monoclinic phase of nanocrystalline $ZrO_2$. $f_t$ is the relative intensity of metastable tetragonal $ZrO_2$. The vertical lines marked ''cryst'' give the values of $\nu_q$, $\eta$, and $\delta$ of $^{181}$Ta in the monoclinic phase of coarse-grained $ZrO_2$. The topmost section of the figure shows the relative intensity $f_m$ of the monoclinic phase and the mean crystallite diameter $d$ obtained from x-ray diffraction [open symbols, present specimen; solid symbols, specimen without preannealing according to previous studies (Ref. 2)].

ber of different surface configurations results in a strong frequency distribution. As pointed out in Ref. 15, the standard PAC analysis as applied here overestimates the asymmetry parameter in the presence of strong frequency distributions. The increase of the asymmetry in $n$-$ZrO_2$ is therefore to a large extent an artifact of the analysis reflecting the increased width of the frequency distribution.

*Component No. 3 (tetragonal phase):* Although the main features of the PAC spectra are determined by the components Nos. 1 and 2, the admission of a weak third component leads to improved fits, in particular for intermediate temperatures $T_A = 900-1000$ K. This component consists of a periodic almost undamped oscillation (strong solid line in Fig. 1) and characterizes probes in the regular tetragonal lattice of $ZrO_2$ stabilized at room temperature. This assignment is based on the value of the quadrupole frequency $\nu_q = 1200$ MHz (Table I) which is identical to that extrapolated from the high-temperature data of coarse-grained tetragonal ($t$-)$ZrO_2$ measured by Jaeger *et al.*[12] Moreover, the EFG exhibits axial symmetry ($\eta = 0$, Table I) as expected for a tetragonal lattice.

A central result of the present study is the observation of a high degree of disorder in nanocrystalline $ZrO_2$ as reflected by the broad QI distribution of component No. 1 (intensity $f_1 = 57\%$) and the enhanced distribution width of the monoclinic phase (component No. 2).

The disorder reflected by component No. 1 of the PAC spectra cannot be attributed exclusively to PAC probes situ-

ated in the crystallite interfaces. This is concluded first from the x-ray-diffraction spectrum of the specimen in the as-prepared state which shows the presence of monoclinic and tetragonal $ZrO_2$ with relative intensities of 65% and 35%, respectively, but contains no evidence for a disordered, e.g., an amorphous grain-boundary phase of substantial intensity. Second, the intensity of the broad component No. 1 is substantially higher than the fraction of 20% atoms located in the two outermost layers of a 14 nm crystallite.

This shows that not only probe sites in the interfacial region, but also those within the crystallites experience a disturbed local environment. It is interesting to note that the local disturbance is apparently more pronounced for the tetragonal than for the monoclinic phase of $n$-$ZrO_2$: Whereas the QI parameters of monoclinic $n$-$ZrO_2$ are rather close to those of the crystalline reference, the fraction of atoms within an undisturbed tetragonal structure derived from the PAC spectra (component No. 3) is much smaller than the intensity of the tetragonal phase in the x-ray-diffraction spectrum (see Table I) and the QI parameters of the dominant component No. 1 differ strongly from those of crystalline $t$-$ZrO_2$.[12]

The difference between the results obtained from PAC spectroscopy and x-ray diffraction on $n$-$ZrO_2$ can be consistently explained by the different sensitivities of the two techniques and, therefore, allows conclusions on the local atomic structure as outlined in the following.

The x-ray-diffraction pattern of $n$-$ZrO_2$ is mainly determined by the Zr sublattice since the atomic number of Zr is much higher than that of O. Owing to its $r^{-3}$ dependence the quadrupole interaction, however, is sensitive mainly to the charges on the nearest-neighbor ($NN$) sites of the probe nucleus. As the $NN$ Zr-O interatomic distances are about 60% shorter than those of the Zr-Zr pairs,[16] the quadrupole interaction primarily reflects the local oxygen environment of the Zr sites and is influenced by neighboring Zr atoms only to a minor extent.

Therefore, the broad QI distribution observed by PAC indicates a wide distribution of Zr-O interatomic distances. Such a disorder of the oxygen sublattice in the $ZrO_2$ nanocrystallites may be caused, e.g., by displacements of oxygen atoms from regular lattice sites and vacant oxygen sites due to oxygen deficiency.[2] In addition, the distribution of Zr-O interatomic distances may partly arise from displacements of Zr atoms from the regular lattice sites of the tetragonal and monoclinic phases which cannot be resolved by x-ray diffraction. Displacements of Zr atoms, e.g., by internal strains which contribute to the broadening of the x-ray-diffraction peaks were observed in a recent high-resolution transmission electron microscopy study.[6] Furthermore, coexisting polymorphs such as cubic or orthorhombic $ZrO_2$ cannot be discerned from the tetragonal phase by x-ray diffraction due to the size-induced broadening of the diffraction peaks. Indications for an orthorhombic phase in $ZrO_2$ powders have recently been found by Winterer *et al.* by means of EXAFS.[4]

### B. Annealing behavior

Figure 2 shows the annealing behavior of the hyperfine parameters and intensity $f_m$ of the monoclinic phase as well as the intensity $f_t$ of the tetragonal phase of $n$-$ZrO_2$. The hyperfine parameters of the tetragonal phase and of the broad component (No. 1, relative intensity $f_1 = 1 - f_m - f_t$) are independent of $T_A$ within the limited experimental accuracy which is caused by the strong correlation between the frequency distribution and the asymmetry. In particular, there are no indications of a decrease of the frequency distribution with temperature. Only the relative intensity decreases with increasing $T_A$ from $f_1 \simeq 0.6(1)$ in the as-prepared sample to reach $f_1 = 0$ at 1400 K.

As a consequence to the preannealing of the $ZrO_2$ specimen, the QI parameters remain constant up to $T_A = 600$ K (Fig. 2). According to x-ray diffraction (Fig. 2 and Refs. 2 and 17) further annealing gives rise to a tetragonal-to-monoclinic phase transition when the crystallite diameter exceeds the critical size of about 10 nm for stabilizing the tetragonal phase. This transition is completed upon annealing at 1200 K as evidenced by measurements of x-ray diffraction on different samples. During this transition, the hyperfine parameters of the monoclinic phase gradually approach those of bulk $m$-$ZrO_2$ as demonstrated by the present PAC study (Fig. 2).

However, even after annealing between $T_A = 1100$ K and 1300 K, where according to the x-ray diffraction the tetragonal-to-monoclinic phase transition is completed,[2,17] the QI parameters ($\nu_q, \eta$) still deviate from those of bulk $m$-$ZrO_2$ and a considerable fraction of PAC probes remains in a disordered environment (intensity $f_1 = 1 - f_m - f_t = 0.38$ of component No. 1; see Fig. 2). This broad component has to be attributed to defects in the crystallites since the intensity $f_1$ is much higher than the volume fraction of crystallite interfaces for crystallite sizes $d > 30$ nm ($T_A > 1100$ K, Ref. 17). The defects as well as the deviations of the QI's from that of the bulk monoclinic phase are stable in this regime of rapidly growing crystallites sizes and, therefore, may be considered as characteristic for the monoclinic nanocrystalline state which is obtained by the transformation from the initial phase with metastable tetragonal structure. Only upon annealing in the high-temperature tetragonal phase, i.e., after a complete martensitic transformation cycle, does the broad component disappear, leading to a PAC spectrum with a pure monoclinic hyperfine pattern ($T_A = 1400$ K, Fig. 2).

Further annealing at 1500 K gives rise to a slight increase of the frequency distribution and a decrease of the quadrupole frequency which might indicate oxygen vacancies caused by the annealing in vacuum.

In summary, we have investigated nanocrystalline $ZrO_2$, produced by gas phase condensation and subsequent oxidation of dc sputtered Zr, by PAC measurements of the electric quadrupole interaction of $^{181}$Ta on Zr sites. In the preannealed specimen ($T_A = 625$ K), where the monoclinic and tetragonal phases coexist, the dominant contribution to the PAC spectrum is characterized by a broad distribution of strong, axially asymmetric electric-field gradients which indicates a highly disordered oxygen environment of the Zr sites. This disorder could not be detected by x-ray diffraction which primarily samples the Zr sublattice. The thermal evolution of the structure and its correlation with the particle size was studied by isochronal annealing up to 1500 K. The disordered tetragonal phase was found to transform mainly

to well-ordered monoclinic $ZrO_2$. Only a minor fraction of the disordered component passes first through the tetragonal phase. A complete defect recovery requires heating and cooling through the high temperature monoclinic-to-tetragonal phase transition at 1400 K.

**ACKNOWLEDGMENTS**

The authors are indebted to Professor Dr. H.-E. Schaefer for discussions. This work was supported by the Deutsche Forschungsgemeinschaft, SFB 408.

[1] M. Mayo, Int. Mater. Rev. **41**, 85 (1996).
[2] R. Würschum, G. Soyez, and H.-E. Schaefer, Nanostruct. Mater. **3**, 225 (1993); in *Structure & Properties of Interfaces in Materials*, edited by W. A. T. Clark, U. Dahman, and C. L. Briant, MRS Symposium Proceedings No. 238 (Materials Research Society, Pittsburgh, 1992), p. 733.
[3] C. A. Melendres, A. Narayanasamy, V. A. Maroni, and R. W. Siegel, J. Mater. Res. **4**, 1246 (1989).
[4] M. Winterer, R. Nitsche, and H. Hahn, Nanostruct. Mater. **9**, 397 (1997).
[5] A. J. Allen, S. Krueger, G. G. Long, H. M. Kerch, H. Hahn , and G. Skanden, Nanostruct. Mater. **7**, 113 (1996).
[6] R. Nitsche, M. Rodewald, G. Skandan, H. Fuess, and H. Hahn, Nanostruct. Mater. **7**, 535 (1996).
[7] R. Würschum, Nanostruct. Mater. **6**, 93 (1995).
[8] P. Sinha and G. S. Collins, Nanostruct. Mater. **3**, 217 (1993).
[9] H. Wolf, H. G. Zimmer, and Th. Wichert, Nanostruct. Mater. **6**, 613 (1995).
[10] St. Lauer, H. Wolf, H. Erhardt, H. G. Zimmer, and Th. Wichert, Hyperfine Interact. **C1**, 262 (1996).
[11] B. Bai and G. S. Collins, Hyperfine Interact. **79**, 761 (1993).
[12] H. Jaeger, J. A. Gardner, J. C. Haygarth, and R. L. Rasera, J. Am. Ceram. Soc. **69**, 458 (1986).
[13] H. Frauenfelder and R. M. Steffen, in *Perturbed Angular Correlations*, edited by E. Karlsson, E. Matthias, and K. Siegbahn (North-Holland, Amsterdam, 1963).
[14] R. Caruso, N. Pellegri, O. de Santis, M. C. Caracoche, and P. C. Rivas, J. Sol-Gel Sci. Technol. **30**, 241 (1994).
[15] M. Forker, Nucl. Instrum. Methods **106**, 121 (1973).
[16] R. Nitsche, M. Winterer, M. Croft, and H. Hahn, Nucl. Instrum. Methods Phys. Res. B **97**, 127 (1995).
[17] U. Brossmann, Ph.D. thesis, Universität Stuttgart, 1998.